

Figure 3 The twitch tension and the resting tension are plotted versus the length of the preparation. Length and radius of curvature are calculated from the height of the bulge using the equations in Fig. 1, panel C. The wall tension is calculated as the product of the pressure and the radius of curvature, preparation from (75/08/21).

1.13 mm, and the wall tension is $T = 1.5 \text{ g/cm}^2 \cdot 0.113 \text{ cm} = 0.175 \text{ g/cm}$. Considering that the layer formed by the myofibrils only averaged approximately $3\mu = 3 \cdot 10^{-4} \text{ cm}$ in width the measured wall tension corresponds to $0.175 \text{ g/cm} / 3 \cdot 10^{-4} = 580 \text{ g/cm}^2$, a value comparable to that obtained from other cardiac tissues.

Figure 3 shows the resting tension and the twitch tension from an experiment where the bulge height was increased, increasing the length of the preparation from 2.8 to 4 mm. Twitch tension develops linearly for approximately 50% of this stretch (from 2.8 to 3.4 mm), plateaus and thereafter decreases linearly for the last 25% of the stretch. The difference between total tension increases rather rapidly in this last segment of the stretch. The difference between total tension and twitch tension is plotted as resting tension in Figure 3. Longer stretches beyond the maximum twitch tension often produce irreversible damage to the single cell layered myocardium. Such stretches lowered the active length-tension curve markedly without altering the passive length tension curve.

The examination of the time course of the developed tension at various muscle lengths consistently showed a prolongation of the time to peak tension with increasing length. The rate of rise also seems to increase with increasing tension. This later observation suggests that stretch increases activation of the myocardium.

The shape of the length-tension curve is quite similar to the length tension curve obtained from a single fiber of frog skeletal muscle (Gordon, Juxley and Julian, J. Physiol. 184, p. 174, 1966). However, since in the present experiment sarcomere length was not measured further analogy with the skeletal muscle observations could be misleading. It is of interest to note that the region of the length-tension curve where active tension is observed (ca. 0.8 l_{max} to ca. 1.5 l_{max}) is only a small fraction of that observed in vertebrate skeletal muscle (ca. 0.6 l_{max} to 1.7 l_{max}).

Comparison of the length-tension curves obtained in these experiments with those obtained from mammalian ventricular muscle show a marked similarity in the onset and magnitude of the resting tension. In contrast to the linear ascending limb of the length-tension curve obtained with this preparation, the

vertebrate myocardial preparations show considerable curvature. This curvature has been explained on basis of the structural complexity (more than one cell layer and fiber branching) of vertebrate cardiac muscle (Julian, Michael and Sollitt, Circ. Res. 37, p. 299, 1975; and Pollack and Huntsman, Ann. Physiol. 227, p. 383, 1974).

Although present results seem to be qualitatively similar to those of vertebrate skeletal muscle, the measurements of sarcomere length is mandatory for determination of filament overlap for such a comparison. We hope to measure the sarcomere length in this preparation by combining laser diffractive technique with our present system.

Supported by HL 16152 and HL 17702.

3 • 1975

Control of Polar Lobe Formation and Connective Tissue Biosynthesis in Embryos of *Ilyanassa obsoleta*

Gary W. Conrad and Gail L. Pakstis; Division of Biology, Kansas State University

Fertilized eggs of the marine neogastropod mudsnail, *Ilyanassa obsoleta*, form and resorb a series of cytoplasmic protuberances from the vegetal pole of the cell before and during first cleavage. These protuberances, called polar lobes, appear to form by constriction of a band of microfilaments in the cortical cytoplasm of the spherical zygote cell (J. Cell Biol., 5, 228-233, 1973). The factors normally controlling this lobe activity are not known. If polar lobes are removed surgically at the time of first cleavage, the resultant "lobeless" embryos develop during the following week into veliger larvae which, by histological criteria, lack several tissues, e.g., external shell, foot, operculum, heart, intestine, eyes, and statocysts. One property shared by the missing tissues is the synthesis of large amounts of extracellular macromolecules. The purpose of our research has been to 1) elucidate factors controlling polar lobe formation, and 2) determine the degree to which morphogenetic factors in the polar lobe cytoplasm of the fertilized egg subsequently affect synthesis and polymerization of extracellular matrices.

Ilyanassa obsoleta (*Nassarius obsoletus*) was collected on the northeast side of Thompson Island and kept in running sea

An Investigation of Orotic Acid as a Precursor of L-Asparagine in Dogfish (*Squalus acanthias*) and Skate (*Raja ocellata*)

D.A. Cooney, A.M. Guarino, H.N. Jayaram and H.A. Milman, National Institutes of Health

The body fluids and proteins of fish contain L-asparagine but the biochemical route for the synthesis of this amino acid amide is unknown (MDIBL Bulletin 12: 68, 1972; *ibid* 13: 27, 1973). Several possibilities for the acquisition or manufacture of L-asparagine can be considered: 1) L-asparagine is assimilated via the diet; 2) L-asparagine is present in seawater and is taken up via the gills; 3) In vivo, L-aspartyl tRNA is amidated to yield L-asparaginyl tRNA which is utilized for protein synthesis with proteolysis then contributing L-asparagine to body fluids; 4) there is a recondite precursor for the carbon skeleton of L-asparagine. It is to the fourth possibility that the present experiments address themselves. A survey of possible intermediary metabolites was made, specifically of those molecules in which the carbon skeleton of L-asparagine was latent. Of these, orotic acid (Figure 1) was selected for detailed study inasmuch

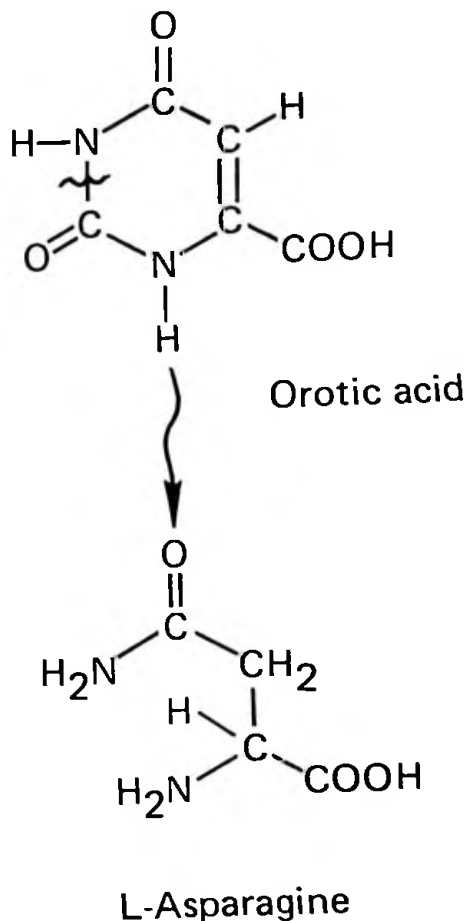


Figure 1

as this molecule contains the entire carbon and nitrogen sequence of L-asparagine. Dogfish were administered a large radioactive bolus (100 μ Ci, 49.1 mCi/mmol) of [$6\text{-}^{14}\text{C}$] orotic acid intravenously followed by measurement of the concen-

water aquaria at MDIBL. Egg capsules were collected from the side of the aquarium and opened with iris scissors. The eggs, which develop synchronously within a single capsule (30-300 eggs/capsule), were suspended in sea water and kept in plastic petri dishes. Eggs develop normally at temperatures below 25° C. For studies of polar lobe formation, solutions were either applied to eggs exogenously or were injected intracellularly by hydrostatic pressure with a Leitz micromanipulator and microinjection apparatus. For studies of glycosaminoglycan biosynthesis, normal and lobeless embryos (500-2,000 embryos/batch) which had developed for 6 days were incubated with $\text{H}_2^{35}\text{SO}_4$ and/or ^3H -glucosamine (100 $\mu\text{C}/\text{ml}$). To monitor structural protein biosynthesis embryos were incubated in presence or absence of β -aminopropionitrile (cross-linking inhibitor) with ^{14}C -proline or ^{14}C -lysine (10 $\mu\text{C}/\text{ml}$). All incubations were for 24 hours at room temperature (18° C). After labeling, embryos were separated from the sea water label solution, rinsed twice with sea water, transferred to 70% ethanol, and taken to dryness. The sea water labeling media, together with the first sea water rinse, were diluted to 80% ethanol (glycosaminoglycans and structural proteins precipitate). Resulting precipitates were washed twice with 80% ethanol, then taken to dryness. Analysis of material in the embryo and sea water precipitates is in progress at Kansas State University.

Treatment of spherical eggs with the divalent cation ionophores, X537A (50 $\mu\text{g}/\text{ml}$) or A23187 (20 $\mu\text{g}/\text{ml}$) in the presence of sea water supplemented with additional Ca (2-10X that in sea water) caused higher percentages of eggs to form polar lobes quickly than did ionophore or additional Ca alone. Solutions of LaCl_3 (5×10^{-2} - 10^{-7} M), in the absence of phosphate and bicarbonate ions, caused no inhibition of polar lobe formation at pH 6.5. At pH 7.3-7.7, however, polar lobe formation could be inhibited by La (5×10^{-3} M). Microinjection of spherical eggs with solutions of CaCl_2 (0.34 - 10^{-4} M) caused very rapid formation of polar lobes. Injection of MgCl_2 (0.5 - 10^{-2} M) also caused lobes to form. Higher concentrations of Mg were required than for Ca, and the lobes took longer to form. Injection of KCl (0.53 - 10^{-4} M) caused few round eggs to form polar lobes; however, when injected into eggs which had already formed a normal polar lobe, a majority of eggs resorbed the lobe very quickly. Such results were predicted on the basis of earlier work (Dev. Biol., 37, 280-294, 1974). Injection of sea water, distilled water, or mineral oil neither caused round eggs to form lobes nor caused eggs with lobes to resorb them. Exogenous solutions of dibutyryl cAMP (5×10^{-3} - 10^{-7} M) had no morphological effect on eggs. Although exogenous solutions of cAMP alone (2.5×10^{-2} - 10^{-7} M) also had no morphological effect on eggs, when such solutions were injected (10^{-5} , 10^{-7} M), a majority of round eggs quickly formed polar lobes. Cyclic GMP, when applied exogenously, (10^{-3} - 10^{-6} M), produced no morphological effect on eggs. Preliminary injection experiments with cGMP (10^{-2} , 10^{-5} M), however, suggested that a significant number of round eggs formed polar lobes as a result of injection.

The results above are consistent with a possible role for intracellular Ca in control of cell shape. (Supported by grant #D07193 from the National Institutes of Health).